THE JOURNAL OF BIOLOGICAL CHEMISTRY VOL. 283, NO. 44, pp. 30151–30163, October 31, 2008

Benzyl Isothiocyanate Targets Mitochondrial Respiratory Chain to Trigger Reactive Oxygen Species-dependent Apoptosis in Human Breast Cancer Cells*

Received for publication, April 1, 2008, and in revised form, August 14, 2008 Published, JBC Papers in Press, September 3, 2008, DOI 10.1074/jbc.M802529200

Dong Xiao, Anna A. Powolny, and Shivendra V. Singh[1]

From the Department of Pharmacology and Chemical Biology, and University of Pittsburgh Cancer Institute, University of Pittsburgh School of Medicine, Pittsburgh, Pennsylvania 15213

Benzyl isothiocyanate (BITC), a dietary cancer chemopreventive agent, causes apoptosis in MDA-MB-231 and MCF-7 human breast cancer cells, but the mechanism of cell death is not fully understood. We now demonstrate that the BITC-induced apoptosis in human breast cancer cells is initiated by reactive oxygen species (ROS) due to inhibition of complex III of the mitochondrial respiratory chain. The BITC-induced ROS production and apoptosis were significantly inhibited by overexpression of catalase and Cu,Zn-superoxide dismutase and pharmacological inhibition of the mitochondrial respiratory chain. The mitochondrial DNA-deficient Rho-0 variant of MDA-MB-231 cells was nearly completely resistant to BITC-mediated ROS generation and apoptosis. The Rho-0 MDA-MB-231 cells also resisted BITC-mediated mitochondrial translocation (activation) of Bax. Biochemical assays revealed inhibition of complex III activity in BITC-treated MDA-MB-231 cells as early as at 1 h of treatment. The BITC treatment caused activation of c-Jun N-terminal kinase (JNK) and p38 mitogen-activated protein kinase (MAPK), which function upstream of Bax activation in apoptotic response to various stimuli. Pharmacological inhibition of both JNK and p38 MAPK conferred partial yet significant protection against BITC-induced apoptosis. Activation of JNK and p38 MAPK resulting from BITC exposure was abolished by overexpression of catalase. The BITC-mediated conformational change of Bax was markedly suppressed by ectopic expression of catalytically inactive mutant of JNK kinase 2 (JNKK2(AA)). Interestingly, a normal human mammary epithelial cell line was resistant to BITC-mediated ROS generation, JNK/p38 MAPK activation, and apoptosis. In conclusion, the present study indicates that the BITC-induced apoptosis in human breast cancer cells is initiated by mitochondria-derived ROS.

Despite significant advances toward targeted therapy and screening techniques, breast cancer continues to claim more than 40,000 lives each year in the United States alone (1). The known risk factors for breast cancer include family history, Li-Fraumeni syndrome, atypical hyperplasia of the breast, late age at first full-term pregnancy, early menarche, and late menopause (2–6). Because some of these risk factors are not easily modifiable (*e.g.* genetic predisposition), other strategies for reduction of breast cancer risk must be considered. Although selective estrogen receptor (ER)[2] modulators (*e.g.* tamoxifen) appear promising for chemoprevention of breast cancer (7–9), this strategy is largely ineffective against ER-negative breast cancer (7, 8). Moreover, the clinical utility of ER antagonists is often limited by side effects (7, 8, 10). Thus, identification of novel agents that are relatively safe but can suppress growth of both ER-positive and ER-negative human breast cancers is highly desirable.

Epidemiological studies continue to support the premise that dietary intake of cruciferous vegetables may lower the risk of various types of malignancies, including breast cancer (11–14). For example, Ambrosone *et al.* (14) observed an inverse correlation between dietary intake of cruciferous vegetables and the risk of breast cancer in premenopausal women in a population-based case control study. The anticarcinogenic effect of cruciferous vegetables is attributed to organic isothiocyanates (ITCs), which are generated upon processing of these vegetables due to hydrolysis of the corresponding glucosinolates through catalytic mediation of myrosinase (15–17). Benzyl-ITC (BITC) is one such compound that has attracted a great deal of research interest because of its remarkable anticancer effects (reviewed in Refs. 15–17). BITC is a potent inhibitor of mammary, lung, and liver carcinogenesis induced by environmental and dietary carcinogens in rodent models (18–20). The *N*-acetylcysteine conjugate of BITC inhibited benzo[*a*]pyrene-induced pulmonary tumorigenesis in A/J mice (21).

In addition to the prevention of chemically induced cancers (18–21), BITC can suppress proliferation of cancer cells in culture by causing cell cycle arrest and/or apoptosis induction (22–27). Elucidation of the mechanism of cellular responses to

* This work was supported, in whole or in part, by National Institutes of Health, NCI, Grants CA129347 and CA101753. The costs of publication of this article were defrayed in part by the payment of page charges. This article must therefore be hereby marked "*advertisement*" in accordance with 18 U.S.C. Section 1734 solely to indicate this fact.

[1] To whom correspondence should be addressed: 2.32A Hillman Cancer Center Research Pavilion, 5117 Centre Ave., Pittsburgh, PA 15213. Tel.: 412-623-3263; Fax: 412-623-7828; E-mail: singhs@upmc.edu.

[2] The abbreviations and trivial name used are: ER, estrogen receptor; ROS, reactive oxygen species; ITC, isothiocyanate; BITC, benzyl isothiocyanate; MRC, mitochondrial respiratory chain; DAPI, 4′,6-diamidino-2-phenylindole; H_2DCFDA, 6-carboxy-2′,7′-dichlorodihydrofluorescein diacetate; Cu,Zn-SOD, copper-zinc superoxide dismutase; COXIV, cytochrome *c* oxidase subunit IV; PARP, poly(ADP-ribose) polymerase; PBS, phosphate-buffered saline; DCF, 2′,7′-dichlorodihydrofluorescein; JNK, c-Jun N-terminal kinase; MAPK, mitogen-activated protein kinase; JNKK2, JNK kinase 2; HMEC, normal human mammary epithelial cell line; CHAPS, 3-[(3-cholamidopropyl)dimethylammonio]-1-propanesulfonic acid; ANOVA, analysis of variance; JC-1, 5,5′,6,6′-tetrachloro-1,1′,3,3′-tetraethylbenzimidazolocarbocyanine iodide.

BITC (cell cycle arrest and apoptosis induction) has been the topic of intense research in the past several years. For example, the BITC-induced apoptosis in leukemia cells correlated with phosphorylation of Bcl-2 and activation of p38 mitogen-activated protein kinase (p38 MAPK) and c-Jun N-terminal kinase (JNK) (24). The cell death caused by BITC in the 1483 human head and neck cancer cell line was regulated by p38 MAPK and extracellular signal-regulated kinase (23). We have shown previously that BITC treatment causes suppression of nuclear factor-κB activation in human pancreatic cancer cells (25). Despite these advances, however, the mechanism by which BITC treatment triggers apoptosis in cancer cells is not fully understood. For example, the signaling intermediates responsible for the initiation of BITC-mediated apoptosis remain to be identified.

We have shown previously that BITC treatment causes caspase-mediated apoptosis in MDA-MB-231 and MCF-7 human breast cancer cells in association with generation of reactive oxygen species (ROS) (27). However, the precise role of ROS in BITC-mediated cell death is unclear. Likewise, the mechanism by which BITC treatment causes ROS generation remains elusive. Here, we demonstrate that BITC treatment inhibits complex III of the mitochondrial respiratory chain (MRC) in breast cancer cells to trigger generation of ROS, which function upstream of JNK and p38 MAPK activation and mitochondrial translocation (activation) of Bax in BITC-induced apoptosis.

EXPERIMENTAL PROCEDURES

Reagents—BITC (purity ~98%) was purchased from Sigma. Reagents for cell culture, including RPMI 1640 medium, penicillin, and streptomycin antibiotic mixture, and fetal bovine serum were purchased from Invitrogen. The 4′,6-diamidino-2-phenylindole (DAPI), rotenone, and diphenyleneiodonium chloride (DPI) were from Sigma, and hydroethidine and 6-carboxy-2′,7′-dichlorodihydrofluorescein diacetate (H_2DCFDA) were from Molecular Probes, Inc. (Eugene, OR). The enzyme-linked immunosorbent assay kit for quantitation of cytoplasmic histone-associated DNA fragmentation was from Roche Applied Science. The anti-cytochrome *c* and anti-Bax 6A7 monoclonal antibodies were from Pharmingen (Palo Alto, CA); antibodies against Bax (polyclonal anti-Bax) and caspase-3 were from Cell Signaling Technology (Danvers, MA); the antibodies against Cu,Zn-superoxide dismutase (Cu,Zn-SOD) and catalase were from Calbiochem; the antibody against cytochrome *c* oxidase subunit IV (COXIV) was from Molecular Probes; the antibodies specific for detection of poly(ADP-ribose) polymerase (PARP), total JNK, phospho-(Thr^{183}/Tyr^{185})-JNK, total p38 MAPK, phospho-(Tyr^{182})-p38 MAPK, and phospho-(Ser63/73)-c-Jun were from Santa Cruz Biotechnology, Inc. (Santa Cruz, CA); and anti-actin antibody was from Oncogene Research Products (San Diego, CA). Pharmacological inhibitors of MAPKs, including SB202190 (p38 MAPK inhibitor) and SP600125 (JNK inhibitor), were purchased from Calbiochem.

Cell Culture and Cell Viability Assay—The human breast cancer cell lines MDA-MB-231 and MCF-7 were procured from the American Type Culture Collection and maintained as described by us previously (27). The normal human mammary epithelial cell line (HMEC) was procured from Lonza (Walkersville, MD) and cultured in epithelial cell basal medium (Lonza). Each cell line was maintained at 37 °C in an atmosphere of 95% air and 5% CO_2. Stock solution of BITC was prepared in Me_2SO, and an equal volume of Me_2SO (final concentration 0.1%) was added to the controls. The effect of BITC treatment on cell viability was determined by trypan blue dye exclusion assay as described by us previously (27).

Ectopic Expression of Catalase and Cu,Zn-SOD by Transient Transfection—The MDA-MB-231 or MCF-7 cells were transiently transfected with the pcDNA3.1 vector encoding catalase or Cu,Zn-SOD or the empty vector (generously provided by Dr. Larry W. Oberley, University of Iowa). Briefly, the cells were seeded in 6-well plates and transfected at 50–70% confluence with pcDNA3.1-catalase, pcDNA3.1-Cu,Zn-SOD, or empty vector using Fugene6 transfection reagent (Roche Applied Sciences) according to the manufacturer's instructions. Twenty-four hours after transfection, the cells were treated with Me_2SO or 2.5 μM BITC for specified time periods. The cells were collected and processed for the desired assays.

Immunoblotting—The cells were treated with BITC as described above, and both floating and attached cells were collected. The cells were lysed as described by us previously (28). The mitochondria-free cytosolic fraction for immunoblotting of cytochrome *c* was prepared as described by us previously (29). The mitochondrial and cytosolic fractions from control and BITC-treated cells for immunoblotting of Bax and cytochrome *c* were prepared using a kit from BioVision (Mountain View, CA), as recommended by the manufacturer. The lysate proteins were resolved by 6–12.5% SDS-PAGE and transferred onto membrane. Immunoblotting was performed as described by us previously (28, 29). The blots were stripped and reprobed with anti-actin antibody to correct for differences in protein loading. Change in protein level was determined by densitometric scanning of the immunoreactive band and corrected for actin loading control. Immunoblotting for each protein was performed at least twice using independently prepared lysates to ensure reproducibility of the results.

ROS Generation Assay—Intracellular ROS generation was measured by flow cytometry following staining with hydroethidine and H_2DCFDA essentially as described by us previously (27). Briefly, 2×10^5 cells were plated in 60-mm culture dishes, allowed to attach by overnight incubation, and exposed to Me_2SO (control) or the desired concentration of BITC for the specified time intervals. The cells were stained with 2 μM hydroethidine and 5 μM H_2DCFDA for 30 min at 37 °C. The cells were collected, and the fluorescence was measured using a Coulter Epics XL flow cytometer. In some experiments, cells were pretreated for specified time periods with rotenone (0.4 μM) or DPI (10 μM) prior to BITC exposure and analysis of ROS generation.

Determination of Apoptosis—Apoptosis induction by BITC was assessed by analysis of cytoplasmic histone-associated DNA fragmentation, which has emerged as a highly sensitive and reliable technique for quantitation of apoptotic cell death. The cytoplasmic histone-associated DNA fragmentation was determined as described by us previously (27). In some experi-

ments, cells were pretreated with rotenone (0.4 μM) or DPI (10 μM) prior to BITC treatment and analysis of cytoplasmic histone-associated DNA fragmentation.

Determination of Caspase-3 Activation—Activation of caspase-3 was determined by flow cytometry using a kit from Cell Signaling Technology. Briefly, the cells (3×10^5) were plated in T25 flasks and allowed to attach by overnight incubation. The cells were then treated with Me_2SO (control) or the desired concentrations of BITC for the specified time periods. Subsequently, the cells were collected by trypsinization and processed for flow cytometric analysis of caspase-3 activation according to the manufacturer's instructions.

Generation of Rho-0 Variant of MDA-MB-231 Cells—The Rho-0 variant of MDA-MB-231 cells was generated and maintained as described previously by King and Attadi (30) with some modifications. Briefly, the cells were cultured in complete medium supplemented with 1 mM sodium pyruvate, 1 mM uridine, and 2.5 μM ethidium bromide for more than 20 passages over a period of 7 weeks. Cells cultured in parallel in medium without ethidium bromide were used as controls (wild-type MDA-MB-231 cells). The cells were washed with phosphate-buffered saline (PBS), trypsinized, and used for different experiments.

Immunocytochemical Analysis for COXIV and Bax—Wild-type and Rho-0 variant of MDA-MB-231 cells (1×10^5) were cultured on coverslips and treated with 2.5 μM BITC or Me_2SO (control) for specified time periods. Cells were treated with 200 nM MitoTracker red at 37 °C for 30 min to stain mitochondria. After washing with PBS, the cells were fixed with 2% paraformaldehyde overnight at 4 °C and permeabilized using 0.1% Triton X-100 in PBS for 10 min. The cells were washed with PBS, blocked with 0.5% bovine serum albumin in PBS for 1 h, and incubated with anti-Bax or anti-COXIV antibody overnight at 4 °C. The cells were then washed with PBS and incubated with Alexa Fluor 488-conjugated secondary antibody (1:1000 dilution; Molecular Probes) for 1 h at room temperature. Subsequently, the cells were washed with PBS and stained with DAPI (10 ng/ml) for 5 min at room temperature. The cells were washed twice with PBS and examined under a Leica fluorescence microscope at ×40 objective lens magnification.

Analysis of Bax Conformation Change—The cells were treated with 2.5 μM BITC or Me_2SO (control) for the specified time interval and lysed using a solution containing 10 mM HEPES (pH 7.4), 150 mM NaCl, 1% CHAPS, and protease inhibitor mixture. Aliquots containing 300 μg of lysate protein were incubated overnight at 4 °C with 4 μg of anti-Bax 6A7 monoclonal antibody. Protein G-agarose beads (50 μl; Santa Cruz Biotechnology) were then added to each sample, and the incubation was continued for an additional 2 h at 4 °C. The immunoprecipitates were washed five times with lysis buffer and subjected to electrophoresis, followed by immunoblotting using polyclonal anti-Bax antibody.

Measurement of MRC Enzyme Activities—Cells were plated at a density of 1×10^6 in 100-mm culture dishes, allowed to attach overnight, and treated with Me_2SO or the desired concentrations of BITC for specified time periods. Cells were then harvested by scraping, washed with PBS, and lysed. Protein concentration was determined using the Bradford reagent. The activity of complex I-linked NADH-ubiquinone oxidoreductase was determined by measuring the reduction of ubiquinone to ubiquinol, which leads to decreased absorbance of NADH at 340 nm. The reaction was initiated by the addition of 50 μM ubiquinone to the reaction mixture containing 100 μg of lysate protein, 20 mM potassium phosphate (pH 7.2), 10 mM $MgCl_2$, 0.15 mM NADH, 0.25% bovine serum albumin, 1 mM KCN at 30 °C. The reaction was monitored for 5 min, and then 10 μM rotenone was added, and the reaction rate was followed for an additional 5 min. The activity of complex I was calculated using the rotenone-sensitive rate and expressed as nmol/min/mg protein. Complex II-linked succinate-ubiquinone oxidoreductase activity was determined by measuring the reduction of 2,6-dichlorophenolindophenol, leading to formation of ubiquinol, which can be monitored at 600 nm. The reaction was initiated by the addition of ubiquinone Q2 to the reaction mixture containing 100 μg of lysate protein, 50 mM potassium phosphate buffer (pH 7.4), 20 mM sodium succinate, 0.1 mM EDTA, 74 μM dichlorophenolindophenol, 1 mM KCN, and 10 μM rotenone and followed for 5 min at 30 °C. 2-Thenoytrifluoroacetone was then added to inhibit the complex II activity. The complex II activity was calculated using the 2-thenoytrifluoroacetone-sensitive rate. Complex III-linked ubiquinol cytochrome *c* reductase activity was determined by monitoring reduction of cytochrome *c* by the electrons donated from ubiquinol, which can be monitored at 550 nm. This is a first order enzymatic reaction, which is dependent on the concentrations of both ubiquinol and cytochrome *c*. The reaction was initiated by the addition of ubiquinol (substrate) to the reaction mixture containing 100 μg of protein lysate, 35 mM potassium phosphate (pH 7.2), 1 mM EDTA, 5 mM $MgCl_2$, 1 mM KCN, 5 μM rotenone, and 15 μM cytochrome *c*. The absorbance of cytochrome *c* was followed at 550 nm for 5 min at 30 °C. The complex III activity was calculated using the pseudo-first order constant, and the results are presented as *K*/min/mg of protein.

Determination of Mitochondrial Membrane Potential—Mitochondrial membrane potential was measured using a potential-sensitive dye, 5,5′,6,6′-tetrachloro-1,1′,3,3′-tetraethylbenzimidazolylcarbocyanine iodide (JC-1) (31). A stock solution of JC-1 (1 mg/ml) was prepared in Me_2SO and freshly diluted with the assay buffer. Briefly, cells (2×10^5) were plated in T25 flasks, allowed to attach by overnight incubation, exposed to the desired concentrations of BITC for the specified time periods, and collected by trypsinization. The cells were incubated with medium containing JC-1 (10 μg/ml) for 15 min at 37 °C. The cells were washed, resuspended in 0.5 ml of assay buffer, and analyzed using a Coulter Epics XL Flow Cytometer. Mitochondrial uncoupler carbonyl cyanide 4-(trifluoromethoxy)phenylhydrazone (25 μM) was used as a positive control.

Genetic Suppression of JNK in MDA-MB-231 Cells—The MDA-MB-231 cells were transiently transfected with the plasmid encoding the catalytically inactive mutant of JNK kinase 2 (JNKK2(AA)) (32), a generous gift from Dr. Michael Karin (University of California at San Diego, La Jolla, CA), or empty pcDNA3.1 vector as described by us previously (33). The cells were then treated with Me_2SO (control) or 2.5 μM BITC for the specified time periods and processed for analysis of DNA frag-

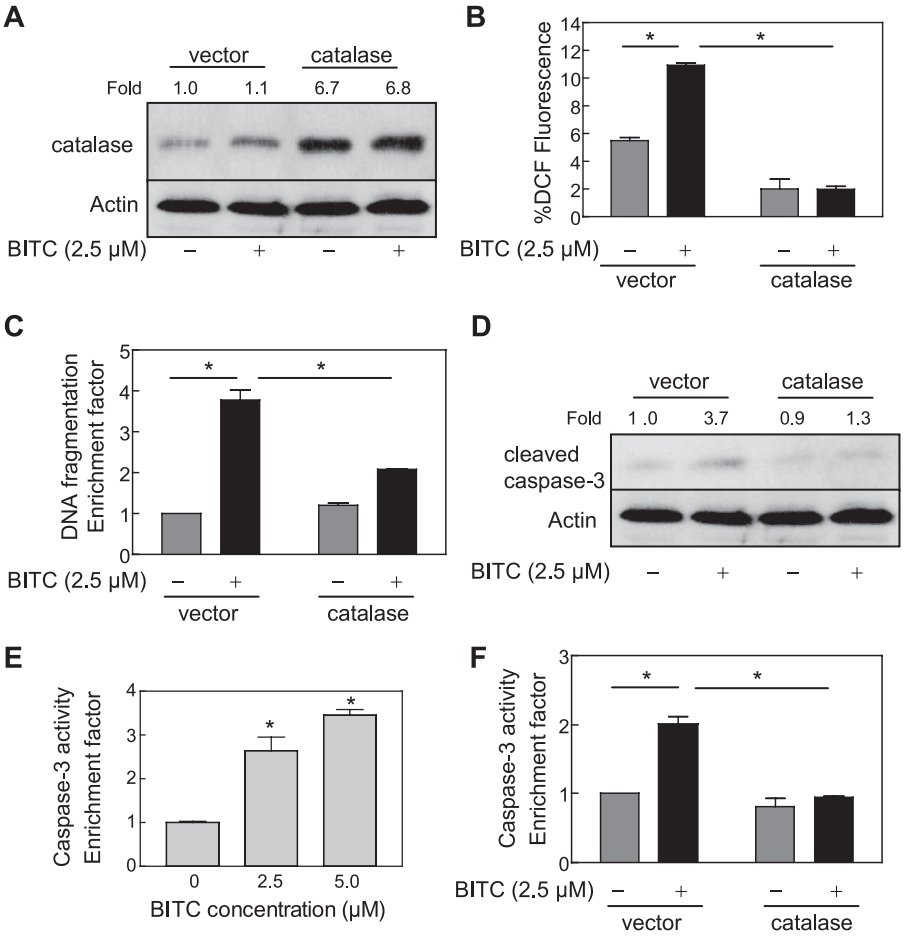

FIGURE 1. **Ectopic expression of catalase conferred protection against BITC-mediated ROS generation and apoptosis in MDA-MB-231 cells.** *A*, immunoblotting for catalase using lysates from MDA-MB-231 cells transiently transfected with the empty pcDNA3.1 vector or pcDNA3.1 vector encoding catalase and treated for 24 h with Me_2SO (control) or 2.5 μM BITC. The blot was stripped and reprobed with anti-actin antibody to ensure equal protein loading. The *numbers above* the immunoreactive bands represent change in protein levels relative to empty vector-transfected control cells treated with Me_2SO (*first lane*). *B*, DCF fluorescence (ROS generation). *C*, cytoplasmic histone-associated DNA fragmentation (results are expressed as enrichment factor relative to Me_2SO-treated empty vector-transfected cells). *D*, cleavage of procaspase-3 in MDA-MB-231 cells transiently transfected with the empty vector or catalase plasmid and treated for 2 h (*B*) or 24 h (*C* and *D*) with Me_2SO (control) or 2.5 μM BITC. In *D*, the *numbers above* the immunoreactive bands represent change in protein level relative to empty vector-transfected control cells treated with Me_2SO (*first lane*). *E*, flow cytometric analysis of caspase-3 activation in untransfected MDA-MB-231 cells treated for 16 h with Me_2SO (control) or the indicated concentrations of BITC. Results are expressed as enrichment factor relative to Me_2SO-treated control. *F*, flow cytometric analysis of caspase-3 activation in MDA-MB-231 cells transiently transfected with the empty vector or catalase plasmid and treated for 24 h with Me_2SO (control) or 2.5 μM BITC. Results are expressed as enrichment factor relative to empty vector-transfected cells treated with Me_2SO. Results in *B*, *C*, *E*, and *F* are mean ± S.E. ($n = 3$). *, significantly different ($p < 0.05$) between the indicated groups by one-way ANOVA followed by Dunnett's (*E*) or Bonferroni's multiple comparison test (*B*, *C*, and *F*). Experiments were performed three times independently with triplicate measurements in each experiment. Similar results were observed in three independent experiments. Representative data from a single experiment are shown.

mentation, immunoblotting for phospho-JNK and phospho-c-Jun or conformational change of Bax.

Statistical Analysis—Statistical significance of difference in measured variables between control and treated groups was determined by *t* test or one-way ANOVA. Difference was considered significant at $p < 0.05$.

RESULTS

BITC-induced Apoptosis in MDA-MB-231 and MCF-7 Cells Was Inhibited by Ectopic Expression of Catalase—We have shown previously that BITC treatment causes apoptosis in MDA-MB-231 (an estrogen-independent cell line) and MCF-7 (an estrogen-responsive cell line) human breast cancer cell lines in association with ROS generation (27). We also found that the BITC-induced apoptosis in both cell lines is significantly inhibited by pretreatment with a combined mimetic of superoxide dismutase and catalase (27). Although these results suggested that ROS might be critical signaling intermediates in BITC-mediated apoptosis, caution must be exercised in interpretation of results using small molecules due to the possibility of an off-target effect(s). To rule out this possibility, we determined the effect of ectopic expression of antioxidative enzyme catalase on ROS generation and apoptosis induction by BITC. As can be seen in Fig. 1*A*, the level of catalase protein was >6-fold higher in MDA-MB-231 cells transiently transfected with pcDNA3.1 vector encoding catalase compared with cells transfected with the empty vector. In addition, BITC treatment (2.5 μM, 24 h) did not have any appreciable effect on levels of endogenous (empty vector-transfected cells) or overexpressed catalase protein (Fig. 1*A*). Similar to untransfected cells (27), the BITC-mediated oxidation of H_2DCFDA to fluorescent 2′,7′-dichlorofluorescein (DCF), a measure of ROS generation (34, 35), was observed in empty vector-transfected MDA-MB-231 cells (Fig. 1*B*). On the other hand, overexpression of catalase conferred complete protection against BITC-mediated oxidation of H_2DCFDA to DCF in MDA-MB-231 cells (Fig. 1*B*). Treatment of empty vector-transfected MDA-MB-231 cells with 2.5 μM BITC for 24 h resulted in an ~4-fold increase in cytoplasmic histone-associated apoptotic DNA fragmentation compared with Me_2SO-treated control cells (Fig. 1*C*). The extent of BITC-mediated cytoplasmic histone-associated DNA fragmentation was significantly lower in catalase-overexpressing MDA-MB-231 cells in comparison with the empty vector-transfected cells (Fig. 1*C*). Consistent with these results, the BITC-mediated cleavage of procaspase-3 was markedly higher in empty vector-transfected MDA-MB-231 cells than in the cells with overexpression of catalase (Fig. 1*D*).

We consistently observed varying levels of basal procaspase-3 cleavage in immunoblotting experiments even in the

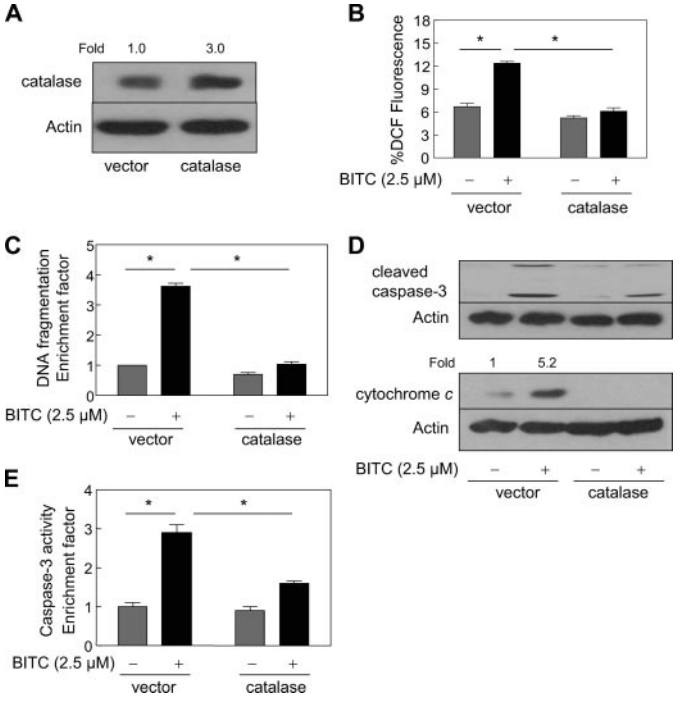

FIGURE 2. **The BITC-mediated ROS generation and apoptosis induction was inhibited by overexpression of catalase in MCF-7 cells.** *A*, immunoblotting for catalase using lysates from MCF-7 cells transiently transfected with the empty pcDNA3.1 vector or vector encoding catalase. The blot was stripped and reprobed with anti-actin antibody to ensure equal protein loading. Change in protein level relative to empty vector-transfected MCF-7 cells is shown *above* the immunoreactive band. *B*, DCF fluorescence (ROS generation); *C*, cytoplasmic histone-associated DNA fragmentation; *D*, cleavage of procaspase-3 and cytosolic release of cytochrome *c*; *E*, activation of caspase-3 in MCF-7 cells transiently transfected with the empty vector or catalase plasmid and treated for 2 h (*B*) or 24 h (*C–E*) with Me_2SO (control) or 2.5 μM BITC. Results in *C* and *E* are expressed as enrichment factor relative to empty vector-transfected cells treated with Me_2SO. Results are mean ± S.E. ($n = 3$). *, significantly different ($p < 0.05$) between the indicated groups by one-way ANOVA followed by Bonferroni's multiple comparison test. *D*, the *numbers above* the immunoreactive bands represent change in protein levels relative to empty vector-transfected control cells treated with Me_2SO. Quantitative results are not shown for cleaved caspase-3, because the band was not detected in empty vector-transfected cells treated with Me_2SO. Experiments were performed three times independently with triplicate measurements in each experiment. Similar results were observed in three independent experiments. Representative data from a single experiment are shown.

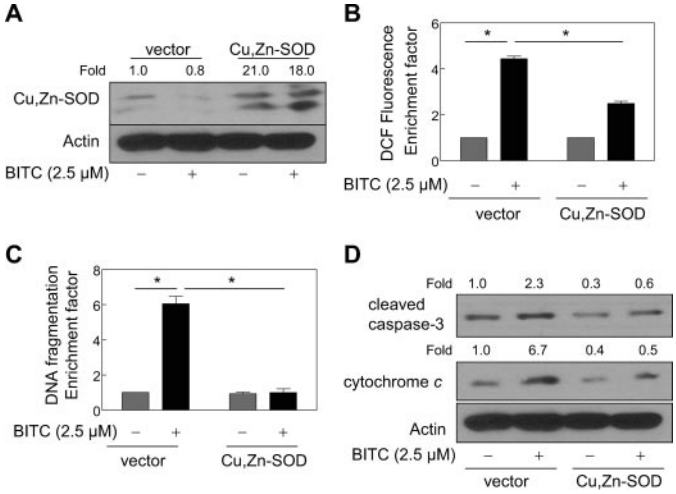

FIGURE 3. **Ectopic expression of Cu,Zn-SOD protected against BITC-mediated ROS generation and apoptosis in MDA-MB-231 cells.** *A*, immunoblotting for Cu,Zn-SOD using lysates from MDA-MB-231 cells transiently transfected with the empty pcDNA3.1 vector or pcDNA3.1 vector encoding Cu,Zn-SOD and treated for 24 h with Me_2SO (control) or 2.5 μM BITC. The blot was stripped and reprobed with anti-actin antibody to ensure equal protein loading. The *numbers above* the immunoreactive bands represent change in protein levels relative to empty vector-transfected cells treated with Me_2SO. *B*, DCF fluorescence (ROS generation); *C*, cytoplasmic histone-associated DNA fragmentation; *D*, cleavage of procaspase-3 and cytosolic release of cytochrome *c* in MDA-MB-231 cells transiently transfected with the empty pcDNA3.1 vector or Cu,Zn-SOD plasmid and treated for 2 h (*B*) or 24 h (*C* and *D*) with Me_2SO (control) or 2.5 μM BITC. In *B* and *C*, results are mean ± S.E. ($n = 3$). *, significantly different ($p < 0.05$) between the indicated groups by one-way ANOVA followed by Bonferroni's multiple comparison test. Experiments were repeated twice with triplicate measurements in each experiment. The results were consistent, and representative data from a single experiment are shown.

absence of BITC treatment, especially in the empty vector-transfected cells (Fig. 1*D*), which may be attributed to endogenous ROS, because this effect was not as pronounced in catalase-overexpressing cells. Although the level of cleaved caspase-3 was consistently higher in empty vector-transfected cells after treatment with BITC compared with the Me_2SO-treated control (Fig. 1*D*), we proceeded to determine the effect of BITC treatment on caspase-3 activity. As shown in Fig. 1*E*, BITC treatment caused activation of caspase-3 in a concentration-dependent manner in untransfected MDA-MB-231 cells, as determined by flow cytometry. Consistent with the immunoblotting data (Fig. 1*D*), the BITC-mediated caspase-3 activation was completely abolished in catalase-overexpressing cells (Fig. 1*F*).

To rule out a possibility that the protective effect of catalase overexpression against BITC-mediated ROS generation and apoptosis was cell line-specific, we carried out similar experiments using MCF-7 cells. Similar to MDA-MB-231 cells (Fig. 1), a 3-fold overexpression of catalase in MCF-7 cells (Fig. 2*A*) afforded marked protection against BITC-mediated (*a*) ROS generation (Fig. 2*B*), (*b*) cytoplasmic histone-associated DNA fragmentation (Fig. 2*C*), (*c*) cleavage of procaspase-3 and release of cytochrome *c* to the cytosol (Fig. 2*D*), and (*d*) activation of caspase-3 (Fig. 2*E*). Collectively, these results indicated that ROS served as critical signaling intermediates in BITC-induced apoptosis in human breast cancer cell lines regardless of their estrogen responsiveness.

Overexpression of Cu,Zn-SOD Conferred Significant Protection against BITC-mediated ROS Generation and Apoptosis in MDA-MB-231 Cells—Superoxide anions are the primary oxygen free radicals produced by the mitochondria and are rapidly removed by conversion to hydrogen peroxide in a reaction catalyzed by SOD (36). To test whether BITC-mediated peroxide production, which was revealed by an increase in DCF fluorescence (Figs. 1*B* and 2*B*), in our model involved superoxide anion production, we determined the effect of ectopic expression of Cu,Zn-SOD on BITC-mediated ROS generation and apoptosis induction using MDA-MB-231 cells. As can be seen in Fig. 3*A*, transient transfection of MDA-MB-231 cells with Cu,Zn-SOD plasmid resulted in an about 21-fold increase in the protein level of Cu,Zn-SOD compared with the empty vector-transfected cells. Similar to catalase (Fig. 1*A*), BITC treatment (2.5 μM, 24 h) did not alter the level of Cu,Zn-SOD protein either in empty vector-transfected cells or in Cu,Zn-SOD-overexpressing MDA-MB-231 cells (Fig. 3*A*). Treatment of empty vector-transfected MDA-MB-231 cells with 2.5 μM BITC for 2 h resulted in an ~4-fold increase in DCF fluorescence, which was

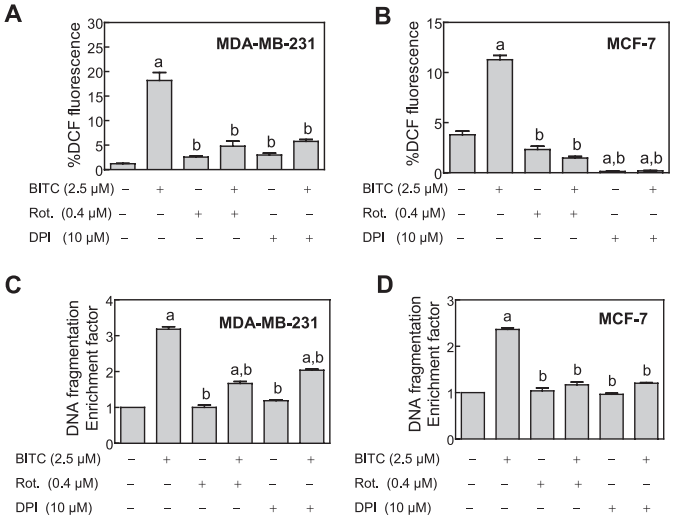

FIGURE 4. **The BITC-mediated ROS generation and apoptosis induction was inhibited in the presence of inhibitors of MRC.** Effect of pretreatment with rotenone and DPI on BITC-mediated ROS generation in MDA-MB-231 cells (*A*) and MCF-7 cells (*B*) and cytoplasmic histone-associated DNA fragmentation in MDA-MB-231 cells (*C*) and MCF-7 cells (*D*). The cells were pretreated for 1–2 h with either Me_2SO (control), 0.4 μM rotenone, or 10 μM DPI. The cells were then either left untreated (Me_2SO, rotenone, and DPI alone control groups) or exposed to 2.5 μM BITC for 1–2 h for analysis of ROS generation and 16–24 h for analysis of cytoplasmic histone-associated DNA fragmentation. Results are mean ± S.E. ($n = 3$); significantly different ($p < 0.05$) compared with Me_2SO-treated control (*a*) and BITC alone treatment group (*b*) by one-way ANOVA followed by Tukey's test. Experiments were performed twice independently with triplicate measurements in each experiment. The results were consistent, and representative data from a single experiment are shown.

reduced partially yet statistically significantly in Cu,Zn-SOD-overexpressing cells (Fig. 3*B*). Ectopic expression of Cu,Zn-SOD also conferred significant protection against BITC-mediated cytoplasmic histone-associated DNA fragmentation (Fig. 3*C*), cleavage of procaspase-3, and cytosolic release of cytochrome *c* (Fig. 3*D*). Together, these results firmly established involvement of ROS in BITC-induced apoptosis in human breast cancer cells.

BITC-induced ROS Generation and Apoptosis Induction in Breast Cancer Cells Was Attenuated by Pretreatment with Inhibitors of MRC—Mitochondria are an important source of cellular ROS, which are generated due to incomplete reduction of oxygen during normal oxidative phosphorylation (37–39). To test whether ROS generation in our model was mitochondria-derived, we determined the effect of MRC inhibitors rotenone and DPI on BITC-mediated ROS generation. Both rotenone and DPI are inhibitors of MRC complex I, whereas DPI can also inhibit other flavoprotein oxidoreductases. As can be seen in Fig. 4, *A* and *B*, the BITC-mediated increase in DCF fluorescence was significantly inhibited in the presence of both rotenone and DPI. In addition, rotenone and DPI treatments conferred significant protection against BITC-mediated cytoplasmic histone-associated DNA fragmentation in both MDA-MB-231 (Fig. 4*C*) and MCF-7 cells (Fig. 4*D*).

Because rotenone and DPI are inhibitors of the MRC, treatment of cells with these agents alone is expected to cause ROS production. For example, MacKenzie *et al.* (40) have shown increased DCF fluorescence in cells exposed to rotenone. To our surprise, ROS production upon treatment with rotenone or DPI alone was either insignificant or not observed at all in MDA-MB-231 (Fig. 4*A*) and MCF-7 cells (Fig. 4*B*). This discrepancy is most likely attributable to differences in cellular models and the experimental conditions between the present work and the MacKenzie study (40). First, the ROS production in the MacKenzie study was observed at 5–25 μM rotenone concentrations (40), which are 12.5–62.5-fold higher than that used in our study (0.4 μM). Second, MacKanzie *et al.* (40) utilized NIH3T3 murine fibroblasts to demonstrate ROS production by rotenone as opposed to the breast cancer cells used in our study. In another study, treatment of HEK293 (a human embryonic kidney cell line) and U87 glioma cells with a very high concentration of rotenone (50 μM) resulted in ROS production (41). On the other hand, in agreement with the results of the present study, the ROS production was minimal in HCT-116 human colon cancer cells exposed to 10 μM DPI (42). Thus, it is reasonable to postulate that the ROS production in response to treatment with rotenone/DPI probably depends upon cell type, concentration of the agent, and treatment duration. Nonetheless, our data suggested that ROS generation upon treatment of human breast cancer cells with BITC might be mitochondria-derived.

Mitochondrial DNA-deficient Rho-0 Variant of MDA-MB-231 Cells Was Resistant toward BITC-mediated Cellular Responses—To firmly establish the contribution of mitochondria in ROS generation by BITC, we generated the Rho-0 variant of MDA-MB-231 cells. Many of the proteins encoded by the mitochondrial DNA are integral components of the MRC complexes (43). The survival of Rho-0 cells is dependent on ATP derived from anaerobic glycolysis, but these cells have functional F1-ATPase (31, 44, 45). The Rho-0 cells lack normal oxidative phosphorylation and are unable to generate ROS from MRC. Initially, we carried out experiments to confirm the Rho-0 phenotype of the variant MDA-MB-231 cells cultured in the presence of 1 mM sodium pyruvate, 1 mM uridine, and 2.5 μM ethidium bromide. Fig. 5*A* depicts morphology of the wild type (cells cultured in parallel in medium without ethidium bromide) and Rho-0 variant of MDA-MB-231 cells. The Rho-0 MDA-MB-231 cells were slightly larger in size with elongated shape and grew at a slower rate compared with wild-type MDA-MB-231 cells. We also stained the wild-type and Rho-0 MDA-MB-231 cells with mitochondria labeling dye MitoTracker red. The mitochondria of Rho-0 cells have altered morphology (46). The mitochondria in wild-type MDA-MB-231 cells were brightly stained with MitoTracker red and COXIV, which is encoded for by the mitochondrial DNA, as revealed by immunofluorescence microscopy (Fig. 5*B*). The intensity of the MitoTracker red and COXIV staining was much weaker in Rho-0 cells than in the wild-type MDA-MB-231 cells (Fig. 5*B*). In addition, the Rho-0 variant of MDA-MB-231 cells exhibited significantly diminished activities of both complex I (Fig. 5*C*) and complex III (Fig. 5*D*) of the MRC. These results confirmed Rho-0 phenotype of the variant MDA-MB-231 cells.

Next, we proceeded to determine the effect of BITC treatment on ROS generation and apoptosis induction using wild-type and Rho-0 MDA-MB-231 cells. As expected, exposure of wild-type MDA-MB-231 cells to 2.5 μM BITC for 1 h resulted in ROS generation, as evidenced by a statistically significant

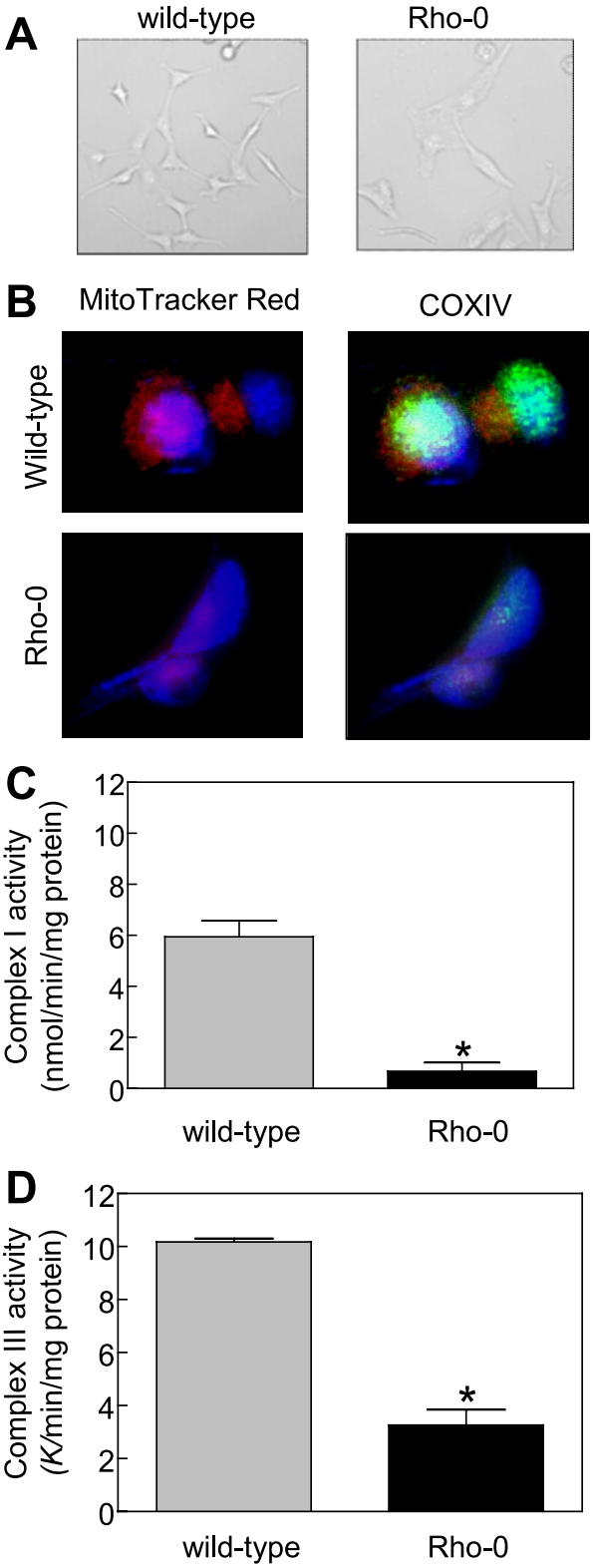

FIGURE 5. **Characterization of Rho-0 variant of MDA-MB-231 cell line.** *A*, morphology of wild-type and Rho-0 MDA-MB-231 cells visualized by microscopy. *B*, fluorescence microscopic analysis of mitochondrial and COXIV staining. The staining for MitoTracker red, COXIV, and nuclei are indicated by *red*, *green*, and *blue fluorescence*, respectively. *C*, activity of complex I using lysate proteins from wild-type and Rho-0 MDA-MB-231 cells. *D*, activity of complex III using lysate proteins from wild-type and Rho-0 MDA-MB-231 cells. Results are mean ± S.E. of 3–5 determinations. *, significantly different ($p < 0.05$) compared with wild-type MDA-MB-231 cells by unpaired *t* test. Each experiment was repeated at least twice, and the results were consistent. Representative data from a single experiment are shown.

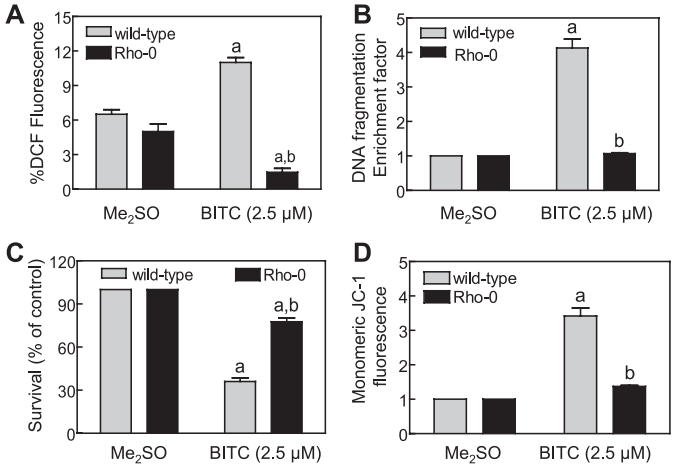

FIGURE 6. **Rho-0 variant of MDA-MB-231 cell line was significantly more resistant to growth suppression and apoptosis induction by BITC compared with wild-type cells.** *A*, analysis of DCF fluorescence (ROS generation) in wild-type and Rho-0 MDA-MB-231 cells following a 1-h treatment with Me_2SO (control) or 2.5 μM BITC. *B*, analysis of cytoplasmic histone-associated DNA fragmentation in wild-type and Rho-0 MDA-MB-231 cells following 24-h treatment with Me_2SO (control) or 2.5 μM BITC. *C*, trypan blue dye exclusion assay to assess cell viability in wild-type and Rho-0 MDA-MB-231 cells following a 24-h treatment with Me_2SO (control) or 2.5 μM BITC. *D*, analysis of mitochondrial membrane potential (monomeric JC-1-associated green fluorescence) in wild-type and Rho-0 MDA-MB-231 cells following a 6-h treatment with Me_2SO (control) or 2.5 μM BITC. Results are mean ± S.E. ($n = 3$); significantly different ($p < 0.05$) compared with corresponding Me_2SO-treated control (*a*) and between BITC-treated wild-type and BITC-treated Rho-0 cells (*b*) by one-way ANOVA followed by Bonferroni's multiple comparison test. Each experiment was performed at least twice with triplicate measurements in each experiment. The results were consistent, and representative data from a single experiment are shown.

increase in DCF fluorescence over Me_2SO-treated control (Fig. 6*A*). Oxidation of H_2DCFDA to DCF was not observed in Rho-0 MDA-MB-231 cells by a similar treatment with BITC (Fig. 6*A*). The BITC treatment (2.5 μM, 24 h) caused an approximately 4-fold increase in cytoplasmic histone-associated DNA fragmentation in the wild-type MDA-MB-231 cells compared with corresponding Me_2SO-treated control (Fig. 6*B*). The cytoplasmic histone-associated DNA fragmentation was marginally affected in Rho-0 MDA-MB-231 cells by a similar BITC treatment (Fig. 6*B*). In agreement with these results, the Rho-0 cells were significantly more resistant to BITC-mediated suppression of cell viability compared with the wild-type MDA-MB-231 cells (Fig. 6*C*).

We have shown previously that BITC treatment causes disruption of the mitochondrial membrane potential in breast cancer cells, as revealed by accumulation of monomeric JC-1 in the cytoplasm (27). The JC-1 dye bearing a delocalized positive charge enters the mitochondrial matrix due to the negative charge established by the intact mitochondrial membrane potential (31). In healthy cells, the JC-1 accumulates in the mitochondria and forms aggregate (red fluorescence). The collapse of the mitochondrial membrane potential is characterized by green fluorescence due to accumulation of monomeric JC-1 in the cytosol (31). We raised the question of whether the BITC-mediated disruption of the mitochondrial membrane potential in human breast cancer cells was caused by ROS generation. To address this question, we determined the effect of BITC treatment on mitochondrial membrane potential using wild-type and Rho-0

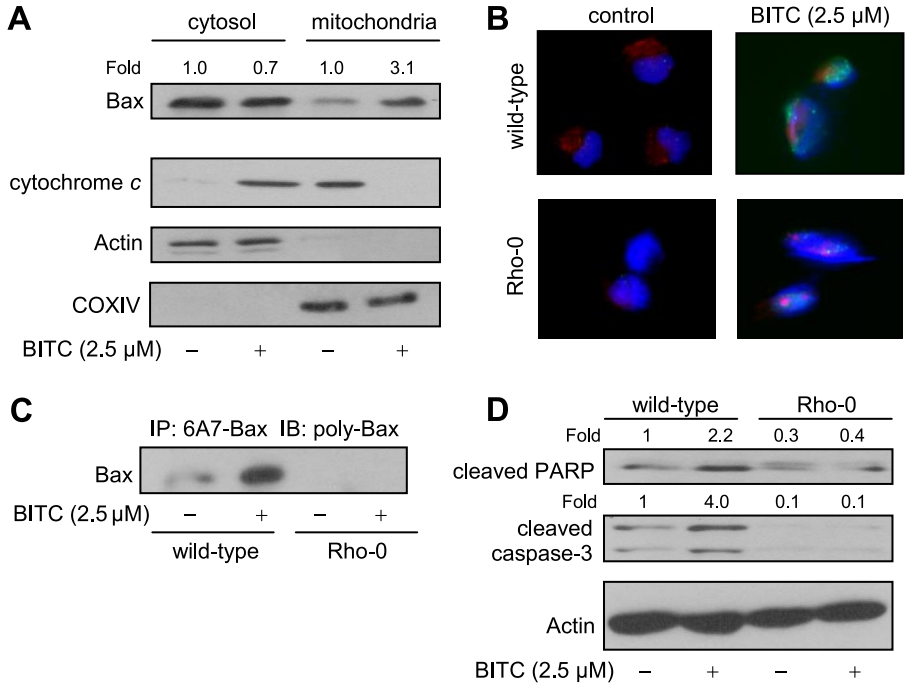

FIGURE 7. **Rho-0 MDA-MB-231 was resistant to BITC-mediated conformational change and mitochondrial translocation of Bax.** *A*, immunoblotting for Bax (using polyclonal anti-Bax antibody) and cytochrome *c* using cytosolic and mitochondrial fractions prepared from MDA-MB-231 cells treated for 16 h with Me_2SO (control) or 2.5 μM BITC. The blots were stripped and reprobed with anti-actin and anti-COXIV antibodies to ensure equal protein loading as well as to rule out cross-contamination of cytosolic and mitochondrial fractions. *B*, immunocytochemical staining for Bax (Bax-associated green fluorescence), mitochondria (MitoTracker red-associated red fluorescence), and nuclei (DAPI-associated blue fluorescence) in wild-type and Rho-0 MDA-MB-231 cells following an 8-h treatment with Me_2SO (control) or 2.5 μM BITC. *C*, analysis of conformational change of Bax using lysates from wild-type and Rho-0 MDA-MB-231 cells treated for 16 h with Me_2SO (control) or 2.5 μM BITC. Bax protein was immunoprecipitated from equal amounts of lysate protein using anti-Bax monoclonal antibody 6A7, which recognizes activated Bax. Immunoprecipitated (*IP*) complexes were subjected to immunoblotting (*IB*) using polyclonal anti-Bax antibody. *D*, immunoblotting for cleaved PARP and cleaved caspase-3 using lysates from wild-type and Rho-0 MDA-MB-231 cells following treatment with Me_2SO (control) or 2.5 μM BITC. The blots were stripped and reprobed with anti-actin antibody to ensure equal protein loading. The *numbers above* the immunoreactive bands represent change in protein levels relative to Me_2SO-treated wild-type MDA-MB-231 cells. Each experiment was performed twice, and the results were comparable. Representative data from a single experiment are shown.

MDA-MB-231 cells. A large fraction of wild-type MDA-MB-231 cells treated for 30 min with 25 μM carbonyl cyanide 4-(trifluoromethoxy)phenylhydrazone (positive control), an uncoupler of mitochondrial oxidative phosphorylation, exhibited monomeric JC-1-associated green fluorescence (results not shown). The BITC treatment (2.5 μM, 6 h) caused a marked increase in monomeric JC-1-associated green fluorescence in wild-type MDA-MB-231 cells, which was much less pronounced in the Rho-0 variant (Fig. 6*D*). Collectively, these results not only confirmed the mitochondrial origin of ROS in BITC-treated breast cancer cells but also indicated that ROS acted upstream of disruption of the mitochondrial membrane potential in the BITC-induced apoptosis cascade.

BITC-mediated ROS Generation Triggered Mitochondrial Translocation of Bax—We have shown previously that SV40 immortalized embryonic fibroblasts derived from Bax and Bak double knock-out mice are significantly more resistant to apoptosis induction by BITC compared with embryonic fibroblasts derived from wild-type mice (27). In normal cells, the multidomain proapoptotic Bcl-2 family member Bax resides in the cytosol but is translocated to the mitochondria upon apoptotic stimuli (47–49). To gain insight into the mechanism downstream of ROS production in BITC-induced apoptosis, we initially determined the effect of BITC treatment on cellular localization of Bax. As shown in Fig. 7*A*, the Bax protein was mainly localized in the cytosol in Me_2SO-treated MDA-MB-231 cells. Treatment of MDA-MB-231 cells with 2.5 μM BITC for 16 h resulted in enrichment of the Bax protein in the mitochondrial fraction with a concomitant decrease in its cytosolic level (Fig. 7*A*). The immunoblotting for cytochrome *c* revealed its localization in the mitochondria in Me_2SO-treated control MDA-MB-231 cells (Fig. 7*A*). The immunostaining for cytochrome *c* in BITC-treated (2.5 μM, 16 h) cells was restricted to the cytosolic fraction. The blots were stripped and reprobed with anti-actin and anti-COXIV antibodies not only to ensure equal protein loading but also to rule out cross-contamination of the cytosolic and mitochondrial fractions (Fig. 7*A*). Next, we studied BITC-mediated translocation of Bax to the mitochondria using wild-type and Rho-0 MDA-MB-231 cells. Fig. 7*B* depicts immunocytochemical analysis of Bax (*green fluorescence*), mitochondria (*red fluorescence*), and nuclei (*blue fluorescence*) in wild-type and Rho-0 MDA-MB-231 cells treated for 8 h with either Me_2SO (control) or 2.5 μM BITC. The Me_2SO-treated wild-type MDA-MB-231 cells exhibited weak Bax-associated green fluorescence but clearly visible mitochondria (*red fluorescence*). The wild-type MDA-MB-231 cells exposed for 8 h to 2.5 μM BITC exhibited an increase in Bax-associated green fluorescence as well as mitochondrial translocation of Bax, as evidenced by the appearance of a *yellow-orange color* due to the merging of MitoTracker red-associated red fluorescence and Bax-associated green fluorescence around DAPI-stained nuclei (Fig. 7*B*). The BITC-mediated induction of Bax or its mitochondrial translocation was not readily evident in Rho-0 MDA-MB-231 cells (Fig. 7*B*).

Because the BITC-mediated translocation of Bax to the mitochondria was not observed in the Rho-0 variant of MDA-MB-231 cells (Fig. 7*B*), we raised the question of whether ROS caused conformational change (activation) of Bax. We addressed this question by immunoprecipitation of active Bax from lysates of control and BITC-treated wild-type and Rho-0 MDA-MB-231 cells using a monoclonal antibody (6A7) that recognizes an epitope at the N terminus of the activated Bax followed by immunoblotting using polyclonal anti-Bax antibody. The BITC-mediated conformational change of Bax was

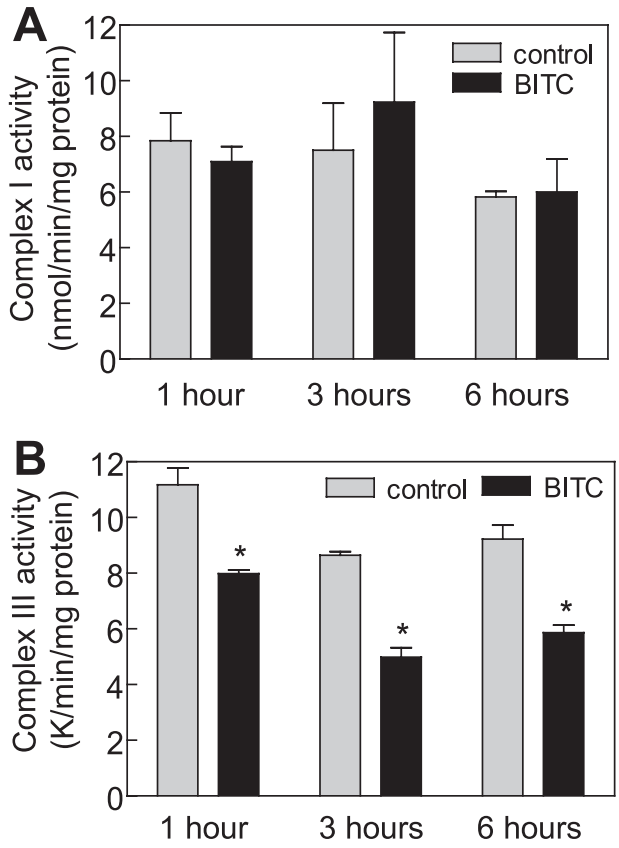

FIGURE 8. **The BITC treatment inhibited complex III activity in MDA-MB-231 cells.** Effect of BITC treatment on complex I-linked NADH ubiquinone oxidoreductase activity (*A*) and complex III-linked ubiquinol cytochrome *c* reductase activity (*B*) in MDA-MB-231 cells. The MDA-MB-231 cells were treated with either Me_2SO (control) or 5 μM BITC for the indicated time periods. Results are mean ± S.E. ($n = 3$). *, significantly different ($p < 0.05$) compared with Me_2SO-treated control by paired *t* test. Experiments were performed three times independently with triplicate measurements in each experiment. Comparable results were observed in each experiment. Representative data from a single experiment are shown.

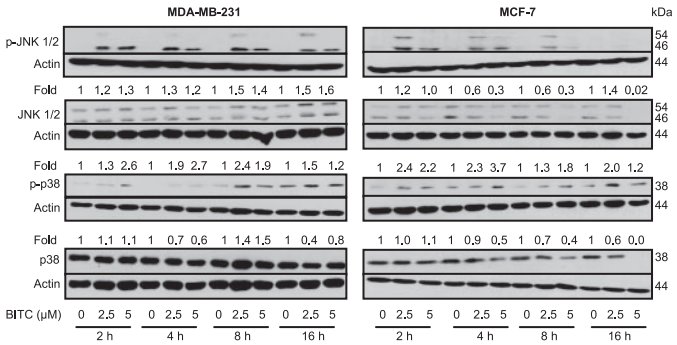

FIGURE 9. **The BITC treatment increased activating phosphorylations of JNK and p38 MAPK in MDA-MB-231 and MCF-7 cells.** Immunoblotting for phospho-JNK, total JNK, phospho-p38 MAPK, and total p38 MAPK using lysates from MDA-MB-231 and MCF-7 cells treated with Me_2SO (control) or 2.5 and 5 μM BITC for the indicated time periods. The blots were stripped and reprobed with anti-actin antibody to ensure equal protein loading. Immunoblotting for each protein was performed twice using independently prepared lysates, and the results were similar. Representative data from a single experiment are shown. -Fold change in phosphoprotein/total protein level relative to Me_2SO-treated control at each time point is shown *above* the immunoreactive band. The quantitative results are not shown for phospho-JNK levels, because the immunoreactive band was not detectable in the Me_2SO-treated controls.

observed in the wild-type cells but not in the Rho-0 MDA-MB-231 cells (Fig. 7*C*). In addition, BITC treatment caused cleavage of procaspase-3 and PARP in wild-type MDA-MB-231 but not in Rho-0 variant (Fig. 7*D*). Collectively, these results indicated that ROS acted upstream of Bax activation in BITC-induced apoptosis.

BITC Treatment Inhibited Complex III Activity of MRC in MDA-MB-231 Cells—To identify the target of BITC-mediated ROS generation, we determined the effect of BITC treatment on activities of MRC enzymes using MDA-MB-231 cells. Complex I (Fig. 8*A*) or complex II activity (results not shown) was not altered upon treatment of MDA-MB-231 with 5 μM BITC. On the other hand, BITC treatment resulted in a statistically significant decrease in activity of complex III of MRC in MDA-MB-231 cells (Fig. 8*B*). These results indicated that BITC treatment inhibited activity of complex III of MRC in MDA-MB-231 cells.

BITC Treatment Caused ROS-dependent Activation of JNK and p38 MAPK in Breast Cancer Cells—The results shown above indicated the critical role of ROS production and Bax activation in BITC-induced apoptosis but did not provide any insight into the signaling pathways linking these effects. Previous studies have implicated stress-activated protein kinases JNK and p38 MAPK in Bax activation by different stimuli, including H_2O_2 (50). Involvement of ROS in activation of Bax has also been suggested in some models of apoptosis (51, 52). Because oxidative stress can activate JNK (33, 53, 54), we raised the question of whether BITC-mediated apoptosis was regulated by ROS-dependent activation of stress-activated protein kinases. Initially, we determined the effect of BITC treatment on activating phosphorylations of JNK and p38 MAPK, and the results are shown in Fig. 9. The BITC treatment increased activating phosphorylations of JNK and p38 MAPK in both MDA-MB-231 and MCF-7 cells, which was not attributable to an increase in their total protein level (Fig. 9). We used pharmacological inhibitors to determine the role of JNK (SP600125) and p38 MAPK (SB202190) in BITC-induced apoptosis. The BITC-induced apoptosis in MDA-MB-231 (Fig. 10*A*) and MCF-7 cell lines (Fig. 10*B*) was partially but significantly inhibited in the presence of both SP600125 and SB202190. Moreover, catalase overexpression conferred marked protection against BITC-mediated activation of both JNK and p38 MAPK (Fig. 10*C*). Collectively, these results pointed toward involvement of ROS in BITC-mediated activation of JNK and p38 MAPK.

BITC-mediated Activation of Bax Was Inhibited by Ectopic Expression of JNKK2(AA)—Next, we raised the question of whether JNK activation contributed to BITC-mediated activation of Bax. We addressed this question by determining the effect of ectopic expression of a catalytically inactive mutant of JNKK2, which is a JNK-specific upstream kinase (32, 55). As can be seen in Fig. 11*A*, BITC treatment (2.5 μM, 8 h) caused an increase in phosphorylations of JNK and its downstream target c-Jun in the empty vector-transfected MDA-MB-231 cells. Ectopic expression of catalytically inactive JNKK2(AA) conferred marked protection against BITC-mediated hyperphosphorylation of both JNK and c-Jun (Fig. 11*A*). A statistically significant increase in cytoplasmic histone-associated DNA fragmentation resulting from 24-h exposure to 2.5 μM BITC

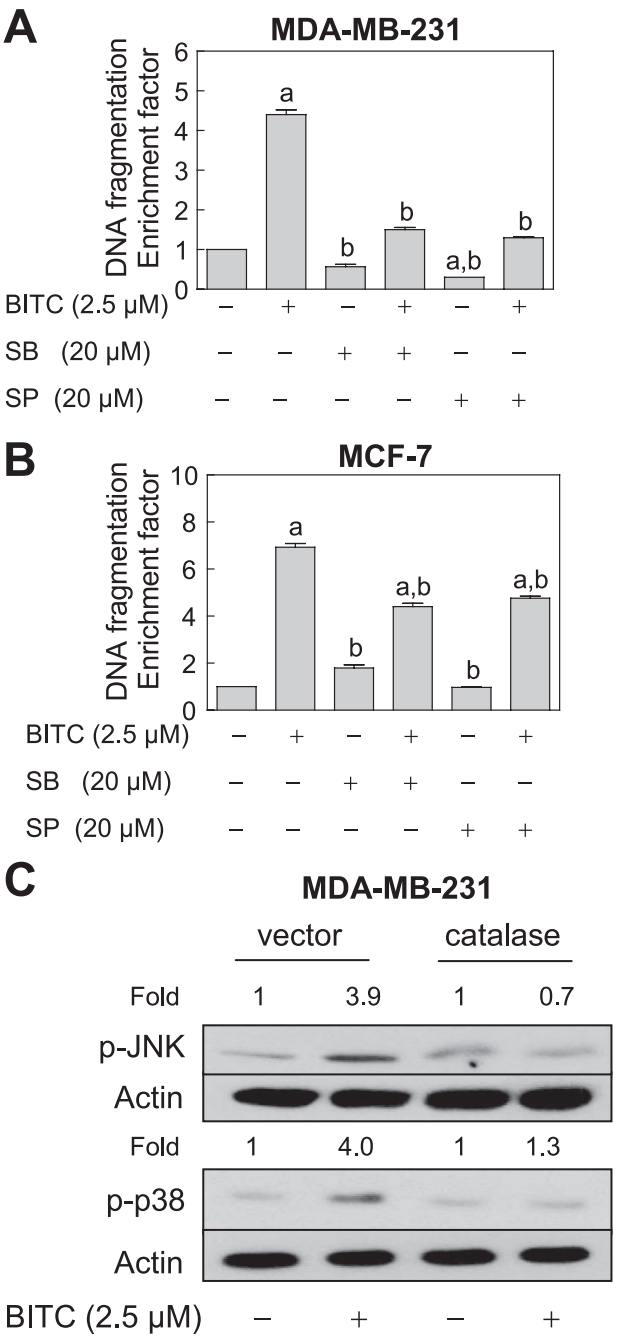

FIGURE 10. **The BITC-induced apoptosis was inhibited by pharmacological inhibition of JNK and p38 MAPK in MDA-MB-231 and MCF-7 cells.** Shown is the effect of pharmacological inhibitors of JNK (SP600125) and p38 MAPK (SB202190) on BITC-induced cytoplasmic histone-associated DNA fragmentation in MDA-MB-231 cells (*A*) and MCF-7 cells (*B*). The cells were pretreated for 2 h with the indicated concentrations of the inhibitors and then exposed to 2. 5 μM BITC for 16 h. Results are mean ± S.E. ($n = 3$); significantly different ($p < 0.05$) compared with Me_2SO-treated control (*a*) and BITC alone (*b*) treatment group by one-way ANOVA followed by Bonferroni's multiple comparison test. Experiments in each cell line were performed twice with triplicate measurements in each experiment. The results of the independent experiments were consistent, and representative data from a single experiment are shown. *C*, immunoblotting for phospho-JNK and phospho-p38 MAPK using lysates from MDA-MB-231 cells transiently transfected with the empty pcDNA3.1 vector or pcDNA3.1 vector encoding catalase and treated for 8 h with Me_2SO (control) or 2.5 μM BITC. The blots were stripped and reprobed with anti-actin antibody to ensure equal protein loading. The *numbers above* the immunoreactive bands represent change in protein levels relative to corresponding Me_2SO-treated control.

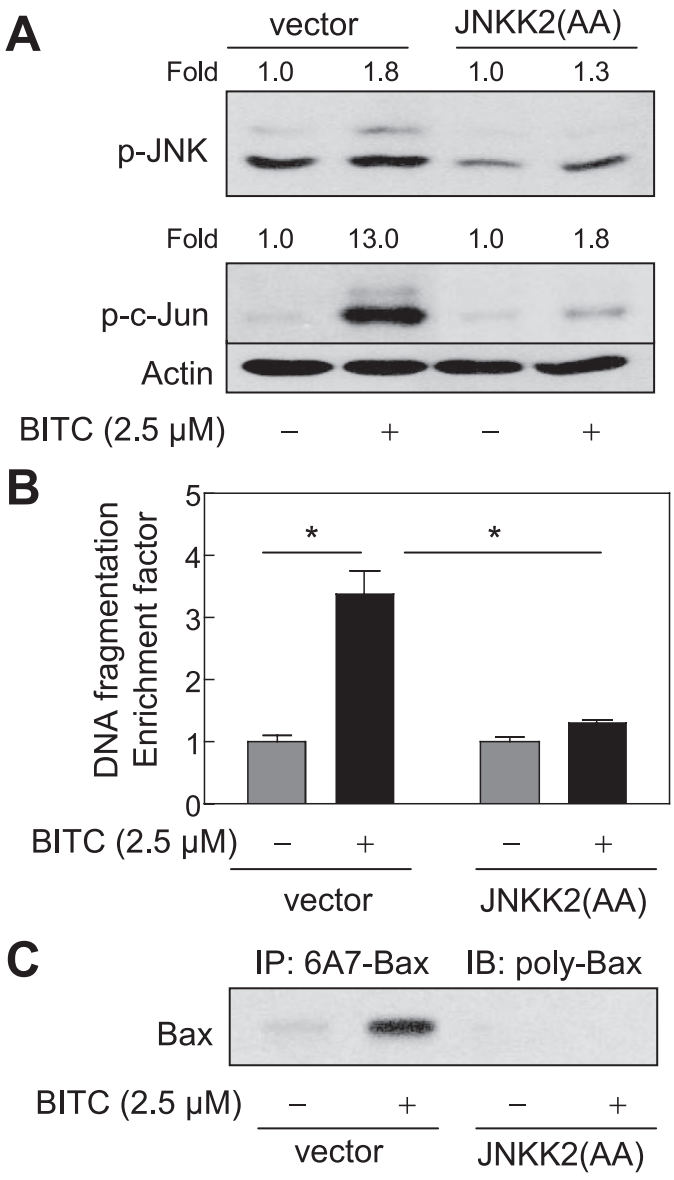

FIGURE 11. **The BITC-induced conformational change of Bax was regulated by JNK signaling axis in MDA-MB-231 cells.** *A*, immunoblotting for phospho-JNK and phospho-c-Jun using lysates from MDA-MB-231 cells transiently transfected with the empty pcDNA3.1 vector or pcDNA3.1 vector encoding a catalytically inactive mutant of JNKK2 (JNKK2(AA)) and treated for 8 h with Me_2SO (control) or 2.5 μM BITC. The blots were stripped and reprobed with anti-actin antibody to ensure equal protein loading. The *numbers above* the immunoreactive bands represent change in protein levels relative to corresponding Me_2SO-treated control. *B*, cytoplasmic histone-associated DNA fragmentation in MDA-MB-231 cells transiently transfected with the empty pcDNA3.1 vector or pcDNA3.1 vector encoding JNKK2(AA) and treated for 24 h with Me_2SO (control) or 2.5 μM BITC. Results are mean ± S.E. ($n = 3$). *, significantly different ($p < 0.05$) between the indicated groups by one-way ANOVA followed by Bonferroni's multiple comparison test. *C*, analysis of conformational change of Bax using lysates from MDA-MB-231 cells transiently transfected with the empty pcDNA3.1 vector or pcDNA3.1 vector encoding JNKK2(AA) and treated for 8 h with Me_2SO (control) or 2.5 μM BITC. Bax protein was immunoprecipitated from equal amounts of lysate proteins using anti-Bax 6A7 monoclonal antibody. The immunoprecipitated complexes were subjected to immunoblotting using anti-Bax polyclonal antibody. Each experiment was repeated twice with comparable results. Representative data from a single experiment are shown.

was observed in the empty vector-transfected MDA-MB-231 cells but not in the MDA-MB-231 cells transiently transfected with JNKK2(AA) (Fig. 11*B*). In addition, overexpression of

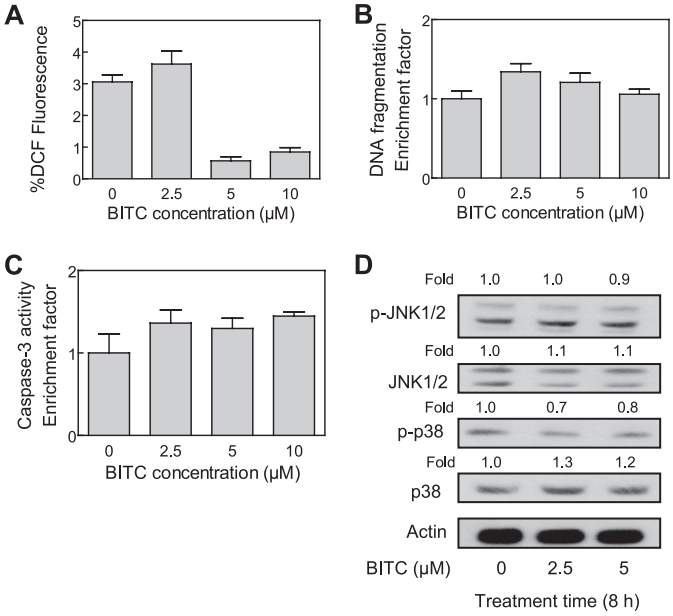

FIGURE 12. **Normal human mammary epithelial cell line HMEC was resistant toward BITC-mediated cellular responses.** Shown is the effect of BITC treatment on ROS production (6-h treatment) (*A*), cytoplasmic histone-associated DNA fragmentation (24-h treatment) (*B*), and activation of caspase-3 (16-h treatment) (*C*) in HMEC cells. Results are mean ± S.E. ($n = 3$). Each assay was performed twice independently with triplicate measurements in each experiment. The results were comparable, and representative data from a single experiment are shown. *D*, immunoblotting for phospho-JNK, total JNK, phospho-p38 MAPK, and total p38 MAPK using lysates from HMEC treated with Me_2SO (control) or 2.5 and 5 μM BITC for 8 h. The blots were stripped and reprobed with anti-actin antibody to ensure equal protein loading. Immunoblotting for each protein was performed twice using independently prepared lysates, and the results were similar. Representative data from a single experiment are shown. -Fold change in phosphoprotein/total protein levels relative to Me_2SO-treated control is shown *above* the immunoreactive band.

JNKK2(AA) conferred protection against BITC-mediated (2.5 μM, 8 h) conformational change of Bax (Fig. 11*C*). Collectively, these results indicated that the BITC-mediated conformational change of Bax was regulated by JNK.

A Normal Human Mammary Epithelial Cell Line Was Resistant toward BITC-mediated Cellular Responses—We raised the question of whether BITC-mediated cellular responses (*e.g.* ROS production, JNK/p38 MAPK activation, and DNA fragmentation) were selective for cancer cells. We used a normal human mammary epithelial cell line, HMEC, to address this question. The BITC treatment (2.5, 5, or 10 μM) did not produce ROS in HMEC (Fig. 12*A*). The HMEC were also resistant toward BITC-induced apoptotic DNA fragmentation (Fig. 12*B*), caspase-3 activation (Fig. 12*C*), and JNK/p38 MAPK activation (Fig. 12*D*). These results indicated that BITC-mediated ROS generation, JNK activation, and apoptosis was selective toward breast cancer cells.

DISCUSSION

The results of the present study demonstrate that ROS act as key signaling intermediates in BITC-mediated apoptosis in human breast cancer cells, which is not a cell line-specific response because the positive correlation between ROS production and cell death is observed in both MDA-MB-231 and MCF-7 cells (Figs. 1–3). The ROS generation and apoptotic DNA fragmentation resulting from BITC exposure are significantly inhibited by overexpression of antioxidative enzymes catalase and Cu,Zn-SOD (Figs. 1–3). These results indicate that ROS serve to initiate the cell death process in these cells. ROS generation by BITC has been documented previously in a rat liver epithelial RL34 cell line (56–58). However, the concentrations of the BITC used to observe ROS generation and apoptosis in RL34 cells (>20 μM) were very high and may not be attainable either by dietary intake of cruciferous vegetables or through pharmacological interventions. The pharmacokinetic parameters for BITC in humans have not yet been determined, but the maximal plasma concentration (C_{max}) of phenethyl-ITC, a close naturally occurring structural analogue of BITC, following ingestion of 100 g of watercress ranged between 673 and 1155 nM (mean of 928 ± 250 nM) (59). A mean C_{max} of 1.04 ± 0.22 μM ITC was reported in another study (60).

Although a possible contribution of ROS in apoptotic response to the ITC family of cancer chemopreventive agents, including phenethyl-ITC, has been suggested previously (27, 61–63), the mechanism of ROS generation by these compounds was not clear. The present study provides convincing experimental evidence to indicate that ROS generation by BITC in human breast cancer cells is mitochondria-derived. This conclusion is supported by the following experimental data: (*a*) the BITC-mediated ROS generation and apoptosis induction are significantly attenuated in the presence of MRC inhibitors rotenone and DPI (Fig. 4); (*b*) the mitochondrial DNA-deficient Rho-0 variant of the MDA-MB-231 cell line is significantly more resistant to ROS generation, growth suppression, and apoptosis induction by BITC compared with wild-type (parental) MDA-MB-231 cells (Fig. 6); (*c*) the BITC treatment causes significant inhibition of complex III activity in MDA-MB-231 cells (Fig. 8); and (*d*) the kinetics of the BITC-mediated ROS generation mirrors inhibition of complex III, both occurring as early as 1 h postexposure (27) (Fig. 8). Although further studies are needed to determine the precise mechanism of BITC-mediated inhibition of complex III activity, it is possible that BITC, being a highly electrophilic molecule (64), covalently modifies critical sulfhydryl groups on a subunit(s) of complex III. In this regard, direct covalent modification of cellular proteins has been suggested to be an important early event in the induction of apoptosis by some ITCs, including phenethyl-ITC (65).

Previous studies have shown that BITC treatment causes inhibition of complex-I-linked state 3 respiration (57, 58). However, inhibition of complex-I-linked state 3 respiration by BITC treatment was observed using rat liver mitochondria and relatively high concentrations of BITC (20–170 μM) (57, 58). It is possible that the inhibitory effect of BITC on MRC is different between normal tissues/cells (*e.g.* rat liver mitochondria (57, 58)) and cancer cells (*e.g.* breast cancer cells used in the present study). At the same time, the possibility that specificity of the BITC-mediated inhibition of MRC is altered in a dose-dependent manner cannot be fully discarded. Further studies are needed to experimentally explore these possibilities.

Another important question relevant to the mechanism of BITC-induced apoptosis in our model relates to the signal transduction downstream of ROS generation. The ROS have been shown to function upstream of cytochrome *c* release and

caspase activation by certain apoptotic stimuli, such as hyperoxia (51). At the same time, the generation of ROS downstream of the release of cytochrome *c* has also been described in some cellular models of mitochondria-mediated apoptosis (66, 67). The present study clearly indicates that ROS act upstream of mitochondrial changes in BITC-induced apoptosis. The BITC-mediated cytosolic release of cytochrome *c* in MDA-MB-231 cells is inhibited by ectopic expression of Cu,Zn-SOD (Fig. 3). The Rho-0 variant of the MDA-MB-231 cell line is also resistant to the BITC-mediated cleavage of PARP and procaspase-3 (Fig. 7*D*). In addition, the BITC-mediated disruption of the mitochondrial membrane potential is obvious in wild-type MDA-MB-231 cells but much less pronounced in its Rho-0 variant (Fig. 6*D*).

We have shown previously that BITC treatment causes induction of multidomain proapoptotic Bcl-2 family members Bax and Bak in MDA-MB-231 and MCF-7 cells (27). In addition, the immortalized mouse embryonic fibroblasts derived from Bax and Bak double knock-out mice are more resistant to BITC-mediated apoptotic cell death compared with embryonic fibroblasts derived from wild-type mice (27). The present study reveals that BITC treatment causes conformational change (activation) and mitochondrial translocation of Bax (Fig. 7, *A–C*). We also found that BITC-mediated activation and mitochondrial translocation of Bax are dependent on ROS generation, because these effects are not observed in the Rho-0 variant of MDA-MB-231 (Fig. 7, *B* and *C*). Previous studies have implicated JNK and p38 MAPK in Bax activation by different stimuli, including H_2O_2 (50). Also, activation of Bax in response to different apoptotic stimuli (*e.g.* hyperoxia) is tightly linked to ROS production. Activation of JNK and p38 MAPK is observed in both MDA-MB-231 and MCF-7 cells upon treatment with BITC (Fig. 9). Moreover, pharmacological inhibition of both JNK and p38 MAPK confers partial but significant protection against BITC-mediated apoptosis in MDA-MB-231 and MCF-7 cells (Fig. 10, *A* and *B*). Ectopic expression of catalase inhibits JNK/p38 MAPK activation caused by BITC treatment (Fig. 10*C*). Furthermore, the BITC-mediated apoptotic DNA fragmentation as well as conformational change of Bax is inhibited by overexpression of a catalytically inactive mutant of JNKK2, which is a JNK-specific kinase. Thus, it is reasonable to conclude that BITC-mediated activation of Bax is regulated by JNK.

Depletion of mitochondrial DNA or treatment with mitochondrial poison has been shown to initiate mitochondrial stress in C2C12 rhabdomyoblasts and A549 human lung carcinoma cells (68). The mitochondrial stress in these cells is characterized by activation of calcineurin and calcium-responsive factors, activation of MAPK, and up-regulation of gene targets involved in regulation of glucose metabolism (*e.g.* hexokinase and pyruvate kinase), oncogenesis (*e.g.* TGFβ1 and cathepsin L), and apoptosis (*e.g.* Bcl-2, Bcl-xL, Bad, and Bax) (68, 69). It is interesting to note that the BITC treatment causes up-regulation, conformation change (activation), and mitochondrial translocation of Bax in wild-type MDA-MB-231 cells but not in its Rho-0 variant (Fig. 7, *B* and *C*). It is possible that the mitochondrial stress induced by BITC treatment is different from that observed in C2C12 rhabdomyblasts and A549 human lung carcinoma cells (68). However, further studies, such as comparison of calcium signaling and analysis of other Bcl-2 family proteins, are needed to substantiate this conclusion.

We also found that a normal human mammary epithelial cell line HMEC is resistant to BITC-mediated ROS generation, apoptotic DNA fragmentation, caspase-3 activation, and activation of JNK and p38 MAPK. These results are consistent with our previous study showing resistance of spontaneously immortalized normal mammary epithelial cell line MCF-10A toward ROS generation and apoptosis induction by BITC treatment (27). Although these observations underscore contribution of ROS and JNK/p38 MAPK in BITC-mediated apoptosis in human breast cancer cells, the mechanism behind resistance of normal mammary epithelial cells to the ROS production by BITC remains to be elucidated.

In conclusion, the present study offers a mechanistic model for BITC-induced apoptosis in human breast cancer cells involving ROS, which are mitochondria-derived and serve to function upstream of JNK/p38 MAPK activation, Bax translocation to the mitochondria, mitochondrial membrane potential collapse, cytosolic release of cytochrome *c*, activation of caspase-3, and DNA fragmentation.

Acknowledgments—We thank Dr. Larry W. Oberley for the generous gifts of catalase and Cu,Zn-SOD plasmids and Dr. Michael Karin for the generous gift of JNKK2(AA) plasmid. The technical assistance of Yan Zeng is also appreciated.

REFERENCES

1. Jemal, A., Siegel, R., Ward, E., Murray, T., Xu, J., Smigal, C., and Thun, M. J. (2006) *CA-Cancer J. Clin.* **56,** 106–130
2. Kelsey, J. L., Gammon, M. D., and John, E. M. (1993) *Epidemiol. Rev.* **15,** 36–47
3. Hulka, B. S., and Stark, A. T. (1995) *Lancet* **346,** 883–887
4. Hankinson, S. E., Willett, W. C., Manson, J. E., Colditz, G. A., Hunter, D. J., Spiegelman, D., Barbieri, R. L., and Speizer, F. E. (1998) *J. Natl. Cancer Inst.* **90,** 1292–1299
5. Cauley, J. A., Lucas, F. L., Kuller, L. H., Stone, K., Browner, W., and Cummings, S. R. (1999) *Ann. Intern. Med.* **130,** 270–277
6. Verloop, J., Rookus, M. A., van der Kooy, K., and van Leeuwen, F. E. (2000) *J. Natl. Cancer Inst.* **92,** 128–135
7. Fisher, B., Costantino, J. P., Wickerham, D. L., Redmond, C. K., Kavanah, M., Cronin, W. M., Vogel, V., Robidoux, A., Dimitrov, N., Atkins, J., Daly, M., Wieand, S., Tan-Chiu, E., Ford, L., Wolmark, N., and other National Surgical Adjuvant Breast and Bowel Project Investigators (1998) *J. Natl. Cancer Inst.* **90,** 1371–1388
8. Cuzick, J., Forbes, J., Edwards, R., Baum, M., Cawthorn, S., Coates, A., Hamed, A., Howell, A., Powles, T., and IBIS Investigators (2002) *Lancet* **360,** 817–824
9. Martino, S., Cauley, J. A., Barrett-Connor, E., Powles, T. J., Mershon, J., Disch, D., Secrest, R. J., Cummings, S. R., and CORE Investigators (2004) *J. Natl. Cancer Inst.* **96,** 1751–1761
10. Braithwaite, R. S., Chlebowski, R. T., Lau, J., George, S., Hess, R., and Col, N. F. (2003) *J. Gen. Intern. Med.* **18,** 937–947
11. Cohen, J. H., Kristal, A. R., and Stanford, J. L. (2000) *J. Natl. Cancer Inst.* **92,** 61–68
12. Kolonel, L. N., Hankin, J. H., Whittemore, A. S., Wu, A. H., Gallagher, R. P., Wilkens, L. R., John, E. M., Howe, G. R., Dreon, D. M., West, D. W., and Paffenbarger, R. S., Jr. (2000) *Cancer Epidemiol. Biomarkers Prev.* **9,** 795–804
13. Fowke, J. H., Chung, F. L., Jin, F., Qi, D., Cai, Q., Conaway, C., Cheng, J. R., Shu, X. O., Gao, Y. T., and Zheng, W. (2003) *Cancer Res.* **63,** 3980–3986

14. Ambrosone, C. B., McCann, S. E., Freudenheim, J. L., Marshall, J. R., Zhang, Y., and Shields, P. G. (2004) *J. Nutr.* **134,** 1134–1138
15. Hecht, S. S. (2000) *Drug Metab. Rev.* **32,** 395–411
16. Talalay, P., and Fahey, J. W. (2001) *J. Nutr.* **131,** 3027s–3033s
17. Conaway, C. C., Yang, Y. M., and Chung, F. L. (2002) *Curr. Drug Metab.* **3,** 233–255
18. Wattenberg, L. W. (1977) *J. Natl. Cancer Inst.* **58,** 395–398
19. Lin, J. M., Amin, S., Trushin, N., and Hecht, S. S. (1993) *Cancer Lett.* **74,** 151–159
20. Sugie, S., Okumura, A., Tanaka, T., and Mori, H. (1993) *Jpn. J. Cancer Res.* **84,** 865–870
21. Yang, Y. M., Conaway, C. C., Chiao, J. W., Wang, C. X., Amin, S., Whysner, J., Dai, W., Reinhardt, J., and Chung, F. L. (2002) *Cancer Res.* **62,** 2–7
22. Zhang, Y., Tang, L., and Gonzalez, V. (2003) *Mol. Cancer Ther.* **2,** 1045–1052
23. Lui, V. W., Wentzel, A. L., Xiao, D., Lew, K. L., Singh, S. V., and Grandis, J. R. (2003) *Carcinogenesis* **24,** 1705–1712
24. Miyoshi, N., Uchida, K., Osawa, T., and Nakamura, Y. (2004) *Cancer Res.* **64,** 2134–2142
25. Srivastava, S. K., and Singh, S. V. (2004) *Carcinogenesis* **25,** 1701–1709
26. Jakubikova, J., Sedlak, J., Bacon, J., Goldson, A., and Bao, Y. (2005) *Int. J. Oncol.* **27,** 1449–1458
27. Xiao, D., Vogel, V., and Singh, S. V. (2006) *Mol. Cancer Ther.* **5,** 2931–2945
28. Xiao, D., Srivastava, S. K., Lew, K. L., Zeng, Y., Hershberger, P., Johnson, C. S., Trump, D. L., and Singh, S. V. (2003) *Carcinogenesis* **24,** 891–897
29. Choi, S., Lew, K. L., Xiao, H., Herman-Antosiewicz, A., Xiao, D., Brown, C. K., and Singh, S. V. (2007) *Carcinogenesis* **28,** 151–162
30. King, M. P., and Attadi, G. (1996) *Methods Enzymol.* **264,** 313–334
31. Cossarizza, A., Baccarani-Contri, M., Kalashnikova, G., and Franceschi, C. (1993) *Biochem. Biophys. Res. Commun.* **197,** 40–45
32. Chen, C. Y., Del Gatto-Konczak, F., Wu, Z., and Karin, M. (1998) *Science* **280,** 1945–1949
33. Antosiewicz, J., Herman-Antosiewicz, A., Marynowski, S. W., and Singh, S. V. (2006) *Cancer Res.* **66,** 5379–5386
34. Rothe, G., and Valet, G. (1990) *J. Leukocyte Biol.* **47,** 440–448
35. Narayanan, P. K., Goodwin, E. H., and Lehnert, B. E. (1997) *Cancer Res.* **57,** 3963–3971
36. Raha, S., and Robinson, B. H. (2001) *Am. J. Med. Genet.* **106,** 62–70
37. Ricci, J. E., Waterhouse, N., and Green, D. R. (2003) *Cell Death Differ.* **10,** 488–492
38. Chandel, N. S., McClintock, D. S., Feliciano, C. E., Wood, T. M., Melendez, J. A., Rodriguez, A. M., and Schumacker, P. T. (2000) *J. Biol. Chem.* **275,** 25130–25138
39. Chandel, N. S., and Schumacker, P. T. (1999) *FEBS Lett.* **454,** 173–176
40. MacKenzie, E. L., Ray, P. D., and Tsuji, Y. (2008) *Free Radic. Biol. Med.* **44,** 1762–1771
41. Chen, Y., McMillan-Ward, E., Kong, J., Israel, S., and Gibson, S. B. (2007) *J. Cell Sci.* **120,** 4155–4166
42. Longpre, J. M., and Loo, G. (2008) *Free Radic. Res.* **42,** 533–543
43. Anderson, S., Bankier, A. T., Barrell, B. G., de Bruijn, M. H., Coulson, A. R., Drouin, J., Eperon, I. C., Nierlich, D. P., Roe, B. A., Sanger, F., Schreier, P. H., Smith, A. J., Staden, R., and Young, I. G. (1981) *Nature* **290,** 457–465
44. King, M. P., and Attardi, G. (1989) *Science* **246,** 500–503
45. Buchet, K., and Godinot, C. (1998) *J. Biol. Chem.* **273,** 22983–22989
46. Gilkerson, R. W., Margineantu, D. H., Capaldi, R. A., and Selker, J. M. (2000) *FEBS Lett.* **474,** 1–4
47. Yamaguchi, H., Chen, J., Bhalla, K., and Wang, H. G. (2004) *J. Biol. Chem.* **279,** 39431–39437
48. Kim, W., Park, W. B., Gao, B., and Jung, M. H. (2004) *Mol. Pharmacol.* **66,** 1383–1396
49. Choi, S., and Singh, S. V. (2005) *Cancer Res.* **65,** 2035–2043
50. Kim, B. J., Ryu, S. W., and Song, B. J. (2006) *J. Biol. Chem.* **281,** 21256–21265
51. Buccellato, L. J., Tso, M., Akinci, O. I., Chandel, N. S., and Budinger, G. R. S. (2004) *J. Biol. Chem.* **279,** 6753–6760
52. Jiang, J., Huang, Z., Zhao, Q., Feng, W., Belikova, N. A., and Kagan, V. E. (2008) *Biochem. Biophys. Res. Commun.* **368,** 145–150
53. Saitoh, M., Nishitoh, H., Fujii, M., Takeda, K., Tobiume, K., Sawada, Y., Kawabata, M., Miyazono, K., and Ichijo, H. (1998) *EMBO J.* **17,** 2596–2606
54. Song, J. J., Rhee, J. G., Suntharalingam, M., Walsh, S. A., Spitz, D. R., and Lee, Y. J. (2002) *J. Biol. Chem.* **277,** 46566–46575
55. Wu, Z., Wu, J., Jacinto, E., and Karin, M. (1997) *Mol. Cell. Biol.* **17,** 7407–7416
56. Nakamura, Y., Ohigashi, H., Masuda, S., Murakami, A., Morimitsu, Y., Kawamoto, Y., Osawa, T., Imagawa, M., and Uchida, K. (2000) *Cancer Res.* **60,** 219–225
57. Nakamura, Y., Kawakami, M., Yoshihiro, A., Miyoshi, N., Ohigashi, H., Kawai, K., Osawa, T., and Uchida, K. (2002) *J. Biol. Chem.* **277,** 8492–8499
58. Kawakami, M., Harada, N., Hiratsuka, M., Kawai, K., and Nakamura, Y. (2005) *Biosci. Biotech. Biochem.* **69,** 2439–2444
59. Liebes, L., Conaway, C. C., Hochster, H., Mendoza, S., Hecht, S. S., Crowell, J., and Chung, F. L. (2001) *Anal. Biochem.* **291,** 279–289
60. Ji, Y., and Morris, M. E. (2003) *Anal. Biochem.* **323,** 39–47
61. Xiao, D., Lew, K. L., Zeng, Y., Xiao, H., Marynowski, S. W., Dhir, R., and Singh, S. V. (2006) *Carcinogenesis* **27,** 2223–2234
62. Trachootham, D., Zhou, Y., Zhang, H., Demizu, Y., Chen, Z., Pelicano, H., Chiao, P. J., Achanta, G., Arlinghaus, R. B., Liu, J., and Huang, P. (2006) *Cancer Cell* **10,** 241–252
63. Wu, X. J., and Hua, X. (2007) *Cancer Biol. Ther.* **6,** 646–647
64. Kolm, R. H., Danielson, U. H., Zhang, Y., Talalay, P., and Mannervik, B. (1995) *Biochem. J.* **311,** 453–459
65. Mi, L., Wang, X., Govind, S., Hood, B. L., Veenstra, T. D., Conrads, T. P., Saha, D. T., Goldman, R., and Chung, F. L. (2007) *Cancer Res.* **67,** 6409–6416
66. Gottlieb, E., Vander Heiden, M. G., and Thompson, C. B. (2000) *Mol. Cell. Biol.* **20,** 5680–5689
67. Cai, J., and Jones, D. P. (1998) *J. Biol. Chem.* **273,** 11401–11404
68. Biswas, G., Guha, M., and Avadhani, N. G. (2005) *Gene* (*Amst.*) **354,** 132–139
69. Biswas, G., Anandatheerthavarada, H. K., Zaidi, M., and Avadhani, N. G. (2003) *J. Cell Biol.* **161,** 507–519